2021 60th IEEE Conference on Decision and Control (CDC)
December 13-15, 2021. Austin, Texas

Efficient computations of multi-species mean field games via graph-structured optimal transport

Axel Ringh, Isabel Haasler, Yongxin Chen, and Johan Karlsson

Abstract— **In this work we develop an efficient numerical solution method for solving potential mean field games with multiple species. This is done by using recent developments that connect mean field games and entropy-regularized optimal transport. In particular, we reformulate the original problem as a structured entropy-regularized multi-marginal optimal transport problem, and develop highly efficient methods for solving the latter. Finally, we illustrate the proposed method on a problem with four interacting species, where each of the species has different target objectives.**

I. Introduction

A strong trend today is the emergence of large scale systems where each subsystem belongs to a class of systems. As the systems become larger, more complex, and more important in the society, there is an increasing need for understanding and controlling macroscopic behavior of such systems of systems. For these systems the available control is typically local and must also take into account the constraints and the utility function of the different groups of subsystems.

An important research area for analyzing and controlling such systems is the area of mean field games [9], [21], [33]–[35], [39], i.e., dynamic games where players' actions are negligible to other players at the individual level but significant when aggregated. Many such games are potential games and can be seen as density control problems where the density abides to a controlled Fokker–Planck equation with distributed control [39]. Such control problems have been studied in, e.g., [7], [10], [14]. An important generalization of this is the multi-species setting when the population consists of several different types of agents or species [1], [8], [16], [34], [37], [39].

In parallel to these results, there has been a rapid development of theory related to the optimal transport problem. One influential paper is [4], where it was shown that certain optimal transport problems can be formulated as fluid dynamics problems, which leads to density control problems over the continuity equation. This idea can be generalized to allow for optimal transport problems that have general underlying dynamics [13], [32]. Moreover, a recent development for numerically solving the optimal transport problem is to include entropy regularization, and the resulting problem can then be efficiently solved using Sinkhorn iterations [19], [43]. Interestingly, this entropy regularization is closely related to the fluid dynamics formulation in [4], and corresponds to adding a stochastic term to the particle dynamics, which leads to a controlled Fokker–Planck equation over the density [11].

In this paper we connect these research directions and show how the optimal transport framework can be used to derive efficient methods for mean field type games with general dynamics and multiple species. In particular, we consider the case where each species has a different objective function. The approach builds on formulating the problem as a multi-marginal optimal transport problem, which is structured due to the fact that the dynamics of each species has the Markov property. This structure can be seen by viewing each marginal as a node in a graph, where edges in the graph denote that there is a dependency between the corresponding marginals [29]. This approach has been used before on more basic graph-structures for control [27], estimation [28], and information fusion [22]. Another related work is [6], in which the single species case is considered for agents that follow the dynamics of a first-order integrator. The computational method developed in [6] is based on a variable elimination technique, while we in this work use a belief-propagation-type technique as in [29], [31].

The outline of the paper is as follows: in Section II we briefly review the areas of mean field games, density optimal control, and optimal transport. In Section III we formulate potential multi-species mean field games as structured multi-marginal optimal transport problems and present an efficient algorithm for computing the optimal solution. In Section IV we present a detailed numerical example, and finally in Section V we present conclusions and future directions.

II. Background

In this section we present some background material on mean field games, density optimal control, and optimal transport. The section is also used to set up notation. In particular, note that we use $./$, $\odot$, $\log(\cdot)$, and $\exp(\cdot)$, to denote element-wise division, multiplication, logarithm, and exponential.

A. Mean field games and density optimal control

Consider a time-varying distribution of agents $\rho(t, x)$, for times $t \in [0, 1]$ and states $x \in X \subset \mathbb{R}^n$. Assume that

This work was supported by the Swedish Research Council (VR) under grant 2020-03454, KTH Digital Futures, the NSF under grant 1942523 and 2008513, and the Knut and Alice Wallenberg foundation, Stockholm, Sweden, under grant KAW 2018.0349.

A. Ringh is with the Department of Electronic and Computer Engineering, The Hong Kong University of Science and Technology, Clear Water Bay, Kowloon, Hong Kong, China. eeringh@ust.hk

I. Haasler, and J. Karlsson are with the Division of Optimization and Systems Theory, Department of Mathematics, KTH Royal Institute of Technology, Stockholm, Sweden. haasler@kth.se, johan.karlsson@math.kth.se

Y. Chen is with the School of Aerospace Engineering, Georgia Institute of Technology, Atlanta, GA, USA. yongchen@gatech.edu

each infinitesimal agent obeys the (Itô) stochastic differential equation

$$dx(t) = f(x(t))dt + B(x(t))\big(v(x(t),t)dt + \sqrt{\epsilon}dw\big) \quad (1)$$

subject to the initial condition $x(0) = x_0$, where the latter follows the distribution $\rho(0,x) = \rho_0(x)$. Here, w is a m-dimensional Wiener process. For ease of notation, we will further suppress the explicit dependence on t from the state x and the explicit dependence on x and t from control signal v and (most of the time) from the density ρ. For the dynamics, we assume that f and B are continuously differentiable with bounded derivatives. In this case, under suitable conditions on the (Markovian) feedback v, there exists a unique solution (a.s.) to (1), cf. [23, Thm. V.4.1], [7, pp. 7-8]. In this work, we also assume that the deterministic counterpart to system (1) is controllable in the (rather strong) sense that for all $x_0, x_1 \in X$ and for all $t > 0$ there exists a control signal in $L_2([0,t])$ that transitions the system from the initial state $x(0) = x_0$ to the final state $x(t) = x_1$.

It is well-known that a potential mean field game can be reformulated as an optimal control problem over densities, where the density ρ is the solution of a controlled Fokker-Planck equation. In particular, under suitable regularity conditions [7], [10] this leads to the density optimal control problem [39]

$$\min_{\rho,v} \int_0^1\int_X \frac{1}{2}\|v\|^2\rho dx dt + \int_0^1 F_t(\rho(t,\cdot))dt + G(\rho(1,\cdot)) \quad (2a)$$

$$\text{s.t. } \frac{\partial\rho}{\partial t} + \nabla\cdot((f+Bv)\rho) - \frac{\epsilon}{2}\sum_{i,k=1}^{n}\frac{\partial^2(\sigma_{ik}\rho)}{\partial x_i \partial x_k} = 0 \quad (2b)$$

$$\rho(0,\cdot) = \rho_0, \quad (2c)$$

where $\nabla\cdot$ denotes the divergence of the vector field, $\sigma(x) := B(x)B(x)^T$ where $(\cdot)^T$ denotes the transpose, and F_t and G are functionals on $L_2 \cap L_\infty$. Moreover, we assume that the latter are proper, convex, and lower semicontinuous, and that F_t is piece-wise continuous with respect to t. Note, e.g., that a terminal constraint $\rho(1,\cdot) = \rho_1$ can be imposed by letting G be the indicator function on the singleton $\{\rho_1\}$.

B. Multi-marginal and computational optimal transport

The optimal transport problem is a classical problem in mathematics, which addresses the problem of how to move mass from an initial distribution to a target distribution with minimum cost; for an introduction and overview of the topic, see, e.g., [49]. The multi-marginal optimal transport problem is an extension of the original problem, which seeks a transport plan between several distributions [5], [22], [25], [41], [42], [45], [46]. Here, we will focus on the discrete case, in which the marginal distributions are given by a finite set of nonnegative vectors[1] $\mu_1, \dots, \mu_{\mathcal{T}} \in \mathbb{R}^N_+$. The transport plan, describing how the mass is moved, and the corresponding cost of moving mass, are both represented by $\mathcal{T}$-mode tensors $\mathbf{M}$ and $\mathbf{C}$, respectively. More precisely, the elements $\mathbf{M}_{i_1,\dots,i_{\mathcal{T}}}$ and $\mathbf{C}_{i_1,\dots,i_{\mathcal{T}}}$ corresponds to the transported mass and the cost of moving mass associated with the tuple $(i_1,\dots,i_{\mathcal{T}})$, respectively. The marginal distributions of $\mathbf{M}$ are given by the projections $P_j(\mathbf{M}) \in \mathbb{R}^N_+$, where

$$(P_j(\mathbf{M}))_{i_j} := \sum_{i_1,\dots,i_{j-1},i_{j+1},i_{\mathcal{T}}} \mathbf{M}_{i_1,\dots,i_{\mathcal{T}}}, \quad (3)$$

and similarly we let $P_{j_1,j_2}(\mathbf{M}) \in \mathbb{R}^{N\times N}_+$ denote the bi-marginal projections on the marginals j_1 and j_2 (see, e.g., [29]). In analogy to the classical bi-marginal problem, for given $\mu_1,\dots,\mu_{\mathcal{T}}$ we have that $\mathbf{M}$ is a feasible transport plan if $P_j(\mathbf{M}) = \mu_j$ for $j = 1,\dots,\mathcal{T}$. A generalization of this, which will be used throughout, is to not necessarily impose marginal constraints on all projections $P_j(\mathbf{M})$, but only for an index set $\Gamma \subset \{1,\dots,\mathcal{T}\}$. The discrete multi-marginal optimal transport problem can thus be formulated as

$$\min_{\mathbf{M}\in\mathbb{R}^{N^{\mathcal{T}}}_+} \quad \langle \mathbf{C}, \mathbf{M}\rangle \quad (4a)$$

$$\text{s.t.} \quad P_j(\mathbf{M}) = \mu_j,\ j \in \Gamma, \quad (4b)$$

where $\langle \mathbf{C},\mathbf{M}\rangle := \sum_{i_1,\dots,i_{\mathcal{T}}} \mathbf{C}_{i_1,\dots,i_{\mathcal{T}}}\mathbf{M}_{i_1,\dots,i_{\mathcal{T}}}$ is the standard inner product. Albeit being a linear program, numerically solving an optimal transport problem can be computationally challenging due to the large number of variables. A popular approach for approximately solving (4) is to perturb the problem by adding the entropy term

$$D(\mathbf{M}) := \sum_{i_1,\dots,i_{\mathcal{T}}} \big(\mathbf{M}_{i_1,\dots,i_{\mathcal{T}}}\log(\mathbf{M}_{i_1,\dots,i_{\mathcal{T}}}) - \mathbf{M}_{i_1,\dots,i_{\mathcal{T}}} + 1\big)$$

to the cost function. First proposed in the bi-marginal setting [19] (see also [43]), the perturbed problem can be solved using so-called Sinkhorn iterations.[2] In particular, defining the tensor $\mathbf{K} = \exp(-\mathbf{C}/\epsilon)$, the optimal transport plan to the perturbed problem can be shown to take the form

$$\mathbf{M} = \mathbf{K} \odot \mathbf{U}, \quad (5)$$

where $\mathbf{U}$ is a rank-one tensor defined by

$$\mathbf{U}_{i_1\dots i_{\mathcal{T}}} = \prod_{j\in\Gamma}(u_j)_{i_j}, \quad (6)$$

see [5], [22]. The Sinkhorn iterations is to iteratively update u_j to match the given marginals, i.e., to iteratively perform

$$u_j \leftarrow u_j \odot \mu_j./P_j(\mathbf{K}\odot\mathbf{U}), \quad \text{for } j \in \Gamma. \quad (7)$$

In fact, the variables u_j correspond to the logarithms of the dual variables in a Lagrangian relaxation of the entropy-regularized version of (4) and the iterations can be viewed as block coordinate ascent in this Lagrangian dual [22], [36], [40], or as iterative Bregman projections [5], [38], [48]. Any of the two viewpoints can be used to show that the iterations converges (linearly) to an optimal solution of the perturbed problem [40], [48]. However, in the multi-marginal case, computing $P_j(\mathbf{K}\odot\mathbf{U})$ is challenging since

[1] To simplify the notation, we assume that all the marginals have the same number of elements, i.e., $\mu_j \in \mathbb{R}^N$. This can easily be relaxed.

[2] In fact, the iterations have been discovered and rediscovered in different settings; see, e.g., [15] for a review of the history.

the number of terms in the sum grows exponentially with the number of marginals. Nevertheless, in some cases when the underlying cost $\mathbf{C}$ is structured the projections can be computed efficiently. In particular, this is the case for many graph-structures, see [2], [5], [22], [27], [29]–[31], [47].

III. SOLVING MULTI-SPECIES MEAN FIELD GAMES

The idea of considering multi-species mean field games was introduced already in [34], [39]. In the potential multi-species mean field games considered here we have L different populations, each with a distribution ρ_ℓ, and where each infinitesimal agent obeys the dynamics

$$dx_\ell(t) = f(x_\ell)dt + B(x_\ell)\big(v_\ell dt + \sqrt{\epsilon}dw_\ell\big), \tag{8}$$

for $\ell = 1, \dots, L$. In this work, we assume that all populations have the same dynamics. This is an initial, simplifying assumption, which we intend to relax in future work. A potential multi-species mean field game problem can, analogously to the single species game, be formulated as an optimal control problem over densities. The problem of interest here takes the form

$$\min_{\rho,\rho_\ell,v_\ell} \int_0^1\!\!\int_X \sum_{\ell=1}^{L} \frac{1}{2}\|v_\ell\|^2\rho_\ell\, dxdt + \int_0^1 F_t(\rho(t,\cdot))dt + G(\rho(1,\cdot)) + \int_X \sum_{\ell=1}^{L}\left(\int_0^1 \mathcal{F}_\ell(t,x)\rho_\ell(t,x)dt + \mathcal{G}_\ell(x)\rho_\ell(1,x)\right)dx \tag{9a}$$

$$\text{s.t.}\ \frac{\partial \rho_\ell}{\partial t} + \nabla\cdot((f(x)+B(x)v_\ell)\rho_\ell) - \frac{\epsilon}{2}\sum_{i,k=1}^{n}\frac{\partial^2(\sigma_{ik}\rho_\ell)}{\partial x_i\partial x_k} = 0, \quad \ell = 1,\dots L, \tag{9b}$$

$$\rho_\ell(0,\cdot) = \rho_{0,\ell}, \quad \rho(t,x) = \sum_{\ell=1}^{L}\rho_\ell(t,x). \tag{9c}$$

where we assume that $\mathcal{F}_\ell(t,\cdot)$ and $\mathcal{G}_\ell$ are in $L_2 \cap L_\infty$, and $\mathcal{F}_\ell(\cdot,x)$ is piece-wise continuous. Note in particular that the cost functions F_t and G are the ones that connect the different species; for $F_t \equiv 0$, $G \equiv 0$, (9) reduces to L independent single-species problems.

A. Discretizing the single-species problem

In a first instance, we consider the single species problem in (2). In particular, when $F_t \equiv 0, G \equiv 0$, the objective function can be reformulated as the Kullback-Leibler (KL) divergence of the controller process with respect to the Wiener process with initial density ρ_0. To this end, denote the distribution of the controlled process on path space by $\mathcal{P}^v$. By invoking the celebrated Girsanov theorem, we have that

$$\mathrm{KL}(\mathcal{P}^v\|\mathcal{P}^0) = \frac{1}{2\epsilon}\mathbb{E}_{\mathcal{P}^v}\{\int_0^1 \|v\|^2dt\} = \frac{1}{2\epsilon}\int_X\int_0^1 \|v\|^2\rho dtdx,$$

where ρ is the solution to (2b) and (2c), see, e.g., [24, pp. 156-157], [20, p. 321]; see also [6], [11], [14], [26]. To ensure that the above holds, it is important that the noise and control enter the system through the same channel, as in (1). This expression, linking stochastic control and entropy, has led to several novel applications of optimal control [11]–[13], [15]. Moreover, using it the problem (2) can be reformulated as

$$\min_{\mathcal{P}^v} \quad \epsilon\,\mathrm{KL}(\mathcal{P}^v\|\mathcal{P}^0) + \int_0^1 F_t(\mathcal{P}_t^v)dt + G(\mathcal{P}_1^v) \tag{10a}$$

$$\text{s.t.} \quad \mathcal{P}_0^v = \rho_0. \tag{10b}$$

After discretization over space, into the grid points $x_1,\dots,x_N$, and discretization over time, into the time points $0, \Delta t, 2\Delta t, \dots, 1$, where $\Delta t = 1/\mathcal{T}$, the problem reduces to

$$\min_{\substack{\mathbf{M}\in\mathbb{R}_+^{N^{\mathcal{T}+1}},\\ \mu_1,\dots,\mu_{\mathcal{T}}\in\mathbb{R}_+^N}} \quad \langle \mathbf{C},\mathbf{M}\rangle + \epsilon D(\mathbf{M}) + \Delta t\sum_{j=1}^{\mathcal{T}-1}F_j(\mu_j) + G(\mu_{\mathcal{T}}) \tag{11a}$$

$$\text{s.t.} \qquad P_j(\mathbf{M}) = \mu_j,\ j = 1,2,\dots,\mathcal{T}, \tag{11b}$$

$$P_0(\mathbf{M}) = \rho_0, \tag{11c}$$

Here, $\mathbf{M}$ is a nonnegative $(\mathcal{T}+1)$-mode tensor that represents the flow of the agents, and $\mathbf{C}$ is a $(\mathcal{T}+1)$-mode tensor that represents the cost of moving agents. In fact, since at a given time the cost of moving agents depends only on the current time step, the tensor $\mathbf{C}$ takes the form

$$\mathbf{C}_{i_0,\dots,i_{\mathcal{T}}} = \sum_{j=0}^{\mathcal{T}-1} C_{i_j,i_{j+1}}. \tag{12a}$$

where C is a $N\times N$ matrix whose elements C_{ik} are the (optimal) cost of moving mass from discretization point x_i to discretization point x_k in one time step, i.e.,

$$C_{ik} = \begin{cases} \min\limits_{v\in L_2([0,\Delta t])} & \int_0^{\Delta t}\frac{1}{2}\|v\|^2dt \\ \text{s.t.} & \dot{x} = f(x) + B(x)v \\ & x(0) = x_i, \quad x(\Delta t) = x_k. \end{cases} \tag{12b}$$

This optimal control problem can in some cases be solved analytically, e.g., in the linear-quadratic case, but in general one typically need to resort to numerical solution methods. Note however, that the computation of the cost function C can be done off-line before solving (11). Also note that due to the controllability assumption, (12b) is always finite. By allowing the matrices C to have elements with value ∞, this assumption may be relaxed. However, in this case one has to assure that (11) has a feasible solution.

As already indicated by the notation, the discretized problem (11) can be identified as an entropy-regularized multi-marginal optimal transport problem; in fact, more specifically as a tree-structured problem [29] where the underlying tree is a path graph.

B. Discretizing the multi-species problem

Next, we move to the multi-species case. To this end, as noted above, for $F_t \equiv 0$ and $G \equiv 0$ in (9) the problem reduces to L independent single-species problems. By adapting the arguments in the previous section, we therefore arrive at the discrete problem

$$\min_{\substack{\mathbf{M}_\ell,\mu_j,\mu_j^{(\ell)}\\ j=1,\ldots,\mathcal{T}\\ \ell=1,\ldots,L}} \sum_{\ell=1}^{L}\langle \mathbf{C},\mathbf{M}_\ell\rangle + \epsilon D(\mathbf{M}_\ell) + \Delta t\sum_{j=1}^{\mathcal{T}-1} F_j(\mu_j) + G(\mu_{\mathcal{T}})$$

$$+\sum_{\ell=1}^{L}\left(\sum_{j=1}^{\mathcal{T}-1}\langle c_{j,\ell},\mu_j^{(\ell)}\rangle + \langle c_{\mathcal{T},\ell},\mu_{\mathcal{T}}^{(\ell)}\rangle\right) \tag{13a}$$

$$\text{s.t.}\quad P_j(\mathbf{M}_\ell) = \mu_j^{(\ell)},\ j=1,\ldots,\mathcal{T}, \tag{13b}$$

$$P_0(\mathbf{M}_\ell) = \rho_{0,\ell},\ \ell=1,\ldots,L, \tag{13c}$$

$$\sum_{\ell=1}^{L}\mu_j^{(\ell)} = \mu_j,\ j=0,\ldots,\mathcal{T} \tag{13d}$$

where $\mathbf{C}$ still has the form (12). Moreover, the second line in the cost (13a) is the discretization of the second line in (9a). In particular, the integrals over X are inner products with respect to the densities, i.e., $(c_{j,\ell})_k = \Delta t\mathcal{F}_\ell(j\Delta t, x_k)$ for $j=1,\ldots,\mathcal{T}-1$ and $(c_{\mathcal{T},\ell})_k = \mathcal{G}_\ell(x_k)$, for $\ell=1,\ldots,L$.

We now reformulate (13) into one single entropy-regularized multi-marginal transport problem. To this end, consider a transport tensor $\mathbf{M}\in\mathbb{R}^{L\times N\times\cdots\times N}$ that has $\mathcal{T}+2$ modes, and where the element $\mathbf{M}_{\ell,i_0,\ldots,i_{\mathcal{T}}}$ corresponds to the amount of mass of species ℓ that moves along the path $i_0,\ldots,i_{\mathcal{T}}$. Moreover, the additional marginal $\mu_{-1}\in\mathbb{R}_+^L$ represents the total mass of the density for species ℓ, i.e., $(\mu_{-1})_\ell = \sum_{k=1}^N(\mu_0^{(\ell)})_k$ for $\ell=1,\ldots,L$. Note that this construction results in that $P_j(\mathbf{M})$ is the total distribution μ_j at time $j\Delta t$, as defined by (13d). Moreover, the bi-marginal projection $P_{-1,j}(\mathbf{M})$ gives the $L\times N$ matrix consisting of $[\mu_j^{(1)},\ldots,\mu_j^{(L)}]^T$. In fact, the latter means that the constraints on the initial distributions, given in (13c), can be imposed by requiring that $P_{-1,0}(\mathbf{M}) = R^{(-1,0)}$, where the matrix $R^{(-1,0)}\in\mathbb{R}_+^{L\times n}$ is

$$R^{(-1,0)} = [\rho_{0,1},\ldots,\rho_{0,L}]^T.$$

Next, defining the set of matrices $C_j\in\mathbb{R}^{L\times N}$ as

$$C_j = [c_{j,1},\ldots,c_{j,L}]^T,\quad j=1,\ldots,\mathcal{T},$$

the last term in the cost (13a) can be written as $\sum_{j=1}^{\mathcal{T}}\langle C_j, P_{-1,j}(\mathbf{M})\rangle$. Finally, by noting that $\sum_{\ell=1}^L D(\mathbf{M}_\ell) = D(\mathbf{M})$, we can write the problem as

$$\min_{\substack{\mathbf{M},\mu_j\\ j=1,\ldots,\mathcal{T}}} \langle\tilde{\mathbf{C}},\mathbf{M}\rangle + \epsilon D(\mathbf{M}) + \Delta t\sum_{j=1}^{\mathcal{T}-1}F_j(\mu_j) + G(\mu_{\mathcal{T}}) \tag{14a}$$

$$\text{s.t.}\quad P_j(\mathbf{M}) = \mu_j,\quad j=1,\ldots,\mathcal{T}, \tag{14b}$$

$$P_{-1,0}(\mathbf{M}) = R^{(-1,0)} \tag{14c}$$

where

$$\tilde{\mathbf{C}}_{i_{-1},i_0,\ldots,i_{\mathcal{T}}} = \sum_{j=1}^{\mathcal{T}}(C_j)_{i_{-1},i_j} + \sum_{j=0}^{\mathcal{T}-1} C_{i_j,i_{j+1}}. \tag{14d}$$

The problem (14) is a graph-structured entropy-regularized multi-marginal optimal transport problem, but where some of the constraints are imposed on the bi-marginals of the transport plan. Next, we present numerical methods for solving such problems.

C. Numerical method for discretized multi-species problems

A numerical method for solving problems of the form (14), similar in spirit to the Sinkhorn iterations (7), can be derived by considering a Lagrangian dual to (14) and numerically solving the latter via coordinate ascent. Here, we will outline how this can be done by following along the lines of [5], [22], [27], [29], [36]; for details, we refer to [30] and the forthcoming paper [44].

To this end, we introduce the Lagrangian variables λ_j, for $j=1,\ldots,\mathcal{T}$, corresponding to the constraints (14b), and the Lagrangian variable $\Lambda^{-1,0}$ for the bimarginal constraint (14b). Using these, the optimal solution to (14) can be shown to be of the form $\mathbf{M}=\mathbf{K}\odot\mathbf{U}$, where $\mathbf{K}=\exp(-\tilde{\mathbf{C}}/\epsilon)$ and where

$$\mathbf{U}_{\ell,i_0,\ldots,i_{\mathcal{T}}} = (U^{-1,0})_{\ell,i_0}\prod_{j=1}^{\mathcal{T}}(u_j)_{i_j}. \tag{15}$$

In particular, $u_j=\exp(\lambda_j/\epsilon)$, for $j=1,\ldots,\mathcal{T}$, and $U^{-1,0}=\exp(-\Lambda^{-1,0}/\epsilon)$. Moreover, the corresponding Lagrangian dual problem takes the form

$$\underset{\substack{U^{-1,0}\in\mathbb{R}_+^{L\times N},\\ u_j\in\mathbb{R}_+^N, j=1,\ldots,\mathcal{T}}}{\text{maximize}} -\epsilon\langle\mathbf{K},\mathbf{U}\rangle - \sum_{j=1}^{\mathcal{T}-1}(\Delta tF_j)^*(-\epsilon\log(u_j)) \tag{16}$$
$$- G^*\left(-\epsilon\log(u_{\mathcal{T}})\right) + \epsilon\langle\log(U^{-1,0}),R^{-1,0}\rangle$$

where $(\cdot)^*$ denotes the Fenchel conjugate [3, Chp. 13]. Furthermore, under some assumptions on F_j and G, strong duality holds between (14) and (16) cf. [48, Lem. 2.1].[3]

Next, in order to simplify the rest of the exposition, assume that F_j^* and G^* are differentiable on $\mathbb{R}_+^N$. Performing coordinate ascent on (16), we fix all except one (set of) variable and maximinze with respect to that variable. Since the cost function in (16) is concave with respect to all variables, the maximum is where the gradient with respect to the variable is zero, leading to the equations

$$0 = -P_j(\mathbf{K}\odot\mathbf{U}) + \nabla(\Delta tF_j)^*(-\epsilon\log(u_j)), \tag{17a}$$

for $j=1,\ldots,\mathcal{T}-1$,

$$0 = -P_{\mathcal{T}}(\mathbf{K}\odot\mathbf{U}) + \nabla G^*(-\epsilon\log(u_{\mathcal{T}})), \tag{17b}$$

and

$$0 = -P_{-1,0}(\mathbf{K}\odot\mathbf{U}) + R^{(-1,0)}, \tag{17c}$$

respectively. Now, by considering (3) and (15), it can be observed that the projections can be written as

$$P_j(\mathbf{K}\odot\mathbf{U}) = u_j\odot w_j \ \text{ and } \ P_{-1,0}(\mathbf{K}\odot\mathbf{U}) = U^{-1,0}\odot W^{-1,0}$$

[3] One set of such assumptions are that there exists a feasible point $\mathbf{M}>0$ to (14) such that for any non-polyhedral function F_j and G, the marginals corresponding to $\mathbf{M}$ are in the relative interior of the effective domain of the corresponding function. These can be weakened somewhat, see [30, Sec. 4.1] for a more detailed disucssion, in which case the functions used in the example in Section IV also fulfill the assumptions.

for some vectors w_j, $j = 1, \dots, \mathcal{T}$, and some matrix $W^{-1,0}$ that do not depend on u_j and $U_{-1,0}$, respectively; cf. [22], [29]. Moreover, as we will see shortly, these vectors and matrices can be efficiently computed (see Theorem 1). Now, a Sinkhorn-type algorithm is thus obtained by iteratively solving the equations (17a)–(17c). Moreover, under the assumption above for strong duality, and assuming that the functions F_j and G are continuous on their effective domain, iteratively solving the equations (17a)–(17c) is in fact an iterative algorithm that converges to the globally optimal solution of (14) [48, Thm. 3.1].

Remark 1: Note that if a term in the cost function (14a) is split as $F_j(\mu_j) = F_{j,1}(\mu_j) + F_{j,2}(\mu_j)$, then the problem can be rewritten using the term $F_{j,1}(\mu_{j,1}) + F_{j,2}(\mu_{j,2})$ by also replacing the constraint $P_j(\mathbf{M}) = \mu_j$ with $P_j(\mathbf{M}) = \mu_{j,1}$ and $P_j(\mathbf{M}) = \mu_{j,2}$. By repeating the above argument, but where the two constraints are relaxed with the multipliers $\lambda_{j,1}$ and $\lambda_{j,2}$, we obtain a similar expressions for $\mathbf{M}$ and the Lagrangian dual, but where u_j is replaced with the product $u_{j,1} \odot u_{j,2}$. This is useful in cases where the equations (17) are difficult to solve for F_j but fast to solve for $F_{j,1}$ and $F_{j,2}$ separately.

Remark 2: The assumption that F_j^* and G^* are differentiable is essentially equivalent with that F_j and G are strictly convex [3, Cor. 18.12]. This assumption can be relaxed, in which case the gradients in (17) must be replaced by the corresponding subgradients. The nonlinear equations (17) will therefore be replaced by monotone inclusion problems; see, e.g., [3] for more on convex optimization and monotone inclusion problems.

As pointed out in Section II-B, directly computing the projections $P_j(\mathbf{K} \odot \mathbf{U})$, which are needed in (17), is computationally challenging. Nevertheless, problem (14) is a graph-structured multi-marginal optimal transport problem, with underlying graph-structure illustrated in Figure 1a. By adapting the arguments in [30], we have the following result.

Theorem 1 ([30]): Let $\mathbf{K} = \exp(-\tilde{\mathbf{C}}/\epsilon)$, with $\tilde{\mathbf{C}}$ defined as in (14d) and $\epsilon > 0$, and let $\mathbf{U}$ be as in (15). Define $K_j = \exp(-C_j/\epsilon)$, $j = 1, \dots, \mathcal{T}$, and $K = \exp(-C/\epsilon)$, and let

$$\hat{\Psi}_j = \begin{cases} U^{-1,0} K, & j = 1, \\ \left(\hat{\Psi}_{j-1} \odot K_{j-1}\right) \operatorname{diag}(u_{j-1}) K, & j = 2, \dots, \mathcal{T}, \end{cases}$$

and

$$\Psi_j = \begin{cases} K_{\mathcal{T}} \operatorname{diag}(u_{\mathcal{T}}) K^T, & j = \mathcal{T} - 1, \\ (\Psi_{j+1} \odot K_{j+1}) \operatorname{diag}(u_{j+1}) K^T, & j = 0, \dots, \mathcal{T} - 2. \end{cases}$$

Then, the projections of the tensor $\mathbf{K} \odot \mathbf{U}$ needed in (17) are given by

$$P_{-1,0}(\mathbf{K} \odot \mathbf{U}) = U^{-1,0} \odot \Psi_0,$$

$$P_{\mathcal{T}}(\mathbf{K} \odot \mathbf{U}) = u_{\mathcal{T}} \odot \left(\hat{\Psi}_{\mathcal{T}} \odot K_{\mathcal{T}}\right)^T \mathbf{1},$$

$$P_j(\mathbf{K} \odot \mathbf{U}) = u_j \odot \left(\hat{\Psi}_j \odot \Psi_j \odot K_j\right)^T \mathbf{1},$$

for $j = 1, \dots, \mathcal{T} - 1$.

Algorithm 1 Scheme for solving potential multi-species mean field games without fixed final distribution.

Input: Initial guess $u_1, \dots, u_{\mathcal{T}}$, $U^{-1,0}$
```
Update Ψ_{T−1} ← K_T diag(u_T) K^T
for j = T − 2, ..., 0 do
    Update Ψ_j ← (Ψ_{j+1} ⊙ K_{j+1}) diag(u_{j+1}) K^T
end for
while Not converged do
    Update U^{−1,0} ← R^{(−1,0)} ./ Ψ_0
    Update Ψ̂_1 ← U^{−1,0} K
    for j = 1, ..., T − 1 do
        w_j ← (Ψ̂_j ⊙ Ψ_j ⊙ K_j)^T 1
        Update u_j by solving (17a).
        Update Ψ̂_{j+1} ← (Ψ̂_j ⊙ K_j) diag(u_j) K
    end for
    w_T ← (Ψ̂_T ⊙ K_T)^T 1
    Update u_T by solving (17b).
    Update Ψ_{T−1} ← K_T diag(u_T) K^T
    for j = T − 2, ..., 0 do
        Update Ψ_j ← (Ψ_{j+1} ⊙ K_{j+1}) diag(u_{j+1}) K^T
    end for
end while
```
Output: $u_1, \dots, u_{\mathcal{T}}$, $U^{-1,0}$

Summarizing the above derivations, a convergent algorithm for solving discretized potential multi-species mean field game problems, cast on the form (14), is given in Algorithm 1. From the algorithm, it can be seen that one update of all variables u_j, $j = 1, \dots, \mathcal{T}$, and $U^{-1,0}$ requires solving $\mathcal{T}$ nonlinear equations of dimension N and an operation with LN elements, respectively. For computing the corresponding projections needed, all $2\mathcal{T}$ matrices $\hat{\Psi}_j$ and Ψ_j need to be updated once, and each update has complexity $\mathcal{O}(LN^2)$. This can be compared with the (at least) $LN^{\mathcal{T}}$ variables in the primal problem (14). A more detailed account of the computational complexity is deferred to the forthcoming paper [44], cf. [30].

Remark 3: In certain cases it might be of interest to impose terminal distributions on the different species in (9), i.e., to impose $\rho_\ell(1, \cdot) = \rho_{1,\ell}$ for some given distribution $\rho_{1,\ell}$, for $\ell = 1, \dots, L$. In this case, the cost functions G and G_ℓ can be removed, as they will only contribute with a constant value. Moreover, in the reformulation (14) of the corresponding discretized problem, these terminal distributions can be imposed by adding the bi-marginal constraint

$$P_{-1,\mathcal{T}}(\mathbf{M}) = R^{(-1,\mathcal{T})}, \tag{18}$$

where $R^{(-1,\mathcal{T})} = [\rho_{\mathcal{T},1}, \dots, \rho_{\mathcal{T},L}]^T$. The underlying graph-structure for this problem is illustrated in Figure 1b, and by adapting the arguments above, we get that such problems can be solved by Algorithm 2.

IV. Numerical example

In this section we consider a numerical example, consisting of a potential multi-species game with $L = 4$ species and with a 2-dimensional state space. More precisely, the

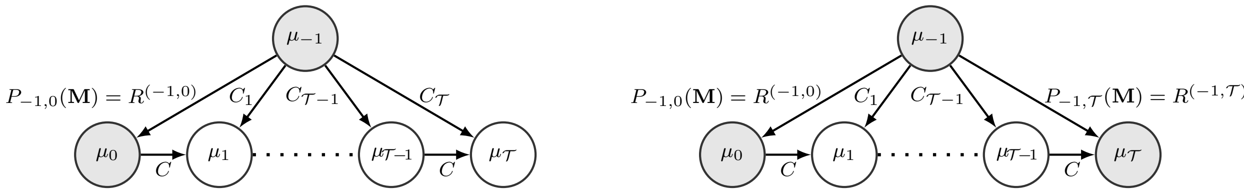

(a) Graph for the multi-species density optimal control problem without fixed final distribution for the different species.

(b) Graph for the multi-species density optimal control problem with fixed final distribution for the different species.

Fig. 1: Illustration of the computational graphs for the multi-species density optimal control problem, with and without fixed final distribution for the different species. Grey circles correspond to known densities, and white circles correspond to densities which are to be optimized over.

Algorithm 2 Scheme for solving potential multi-species mean field games with fixed final distribution.

Input: Initial guess $u_1, \ldots, u_{\mathcal{T}-1}$, $U^{-1,0}$, $U^{-1,\mathcal{T}}$
Update $\Psi_{\mathcal{T}-1} \leftarrow U^{-1,\mathcal{T}} K^T$
Steps 2–12 in Algorithm 1.
    Update $U^{-1,\mathcal{T}} \leftarrow R^{(-1,\mathcal{T})}./\hat{\Psi}_{\mathcal{T}}$
    Update $\Psi_{\mathcal{T}-1} \leftarrow U^{0,\mathcal{T}} K^T$
Steps 16–19 in Algorithm 1.
Output: $u_1, \ldots, u_{\mathcal{T}-1}$, $U^{-1,0}$, $U^{-1,\mathcal{T}}$

densities have support on $[0,3] \times [0,3]$ which we discretize into 100×100 grid points $\{x_{i,k}\}_{i,k=1}^{100}$, i.e., with cell size $\Delta x = 0.03^2$. Moreover, we discretize the time interval into $\mathcal{T}+1 = 40$ time steps, i.e., with a time index $j = 0, \ldots, 39$ and discretization size $\Delta t = 1/39$. We consider the linear-quadratic case, with the dynamics given by $f(x) \equiv 0$ and $B(x) = I$. This means that the cost of moving mass on the discretized grid is constant over time and given by $C = [|x_{i_1,k_1} - x_{i_2,k_2}|^2]_{i_1,i_2,k_1,k_2=1}^{100}$, i.e., corresponding to the squared Wasserstein-2 distance on the discrete 2-dimensional grid. Using this setup, we consider the example

$$\min_{\substack{\mathbf{M}_\ell \in \mathbb{R}_+^{(100^2)^{40}}, \\ \mu_j^{(\ell)} \in \mathbb{R}_+^{100^2}}} \quad \sum_{\ell=1}^{4} \left(\langle \mathbf{C}, \mathbf{M}_\ell \rangle + \epsilon D(\mathbf{M}_\ell) + \sum_{j=1}^{39} \langle \tilde{c}_\ell, \mu_j^{(\ell)} \rangle \right)$$
$$+ 3\|\mu_{19} - \tilde{\mu}_1\|_2^2 + 3\|\mu_{39} - \tilde{\mu}_2\|_2^2 \qquad (19a)$$
$$\text{subject to} \quad P_j(\mathbf{M}_\ell) = \mu_j^{(\ell)}, \quad j = 0, \ldots, 39,$$
$$\ell = 1, 2, 3, 4, \qquad (19b)$$
$$\sum_{\ell=1}^{4} \mu_j^{(\ell)} = \mu_j, \quad j = 0, \ldots, 39, \qquad (19c)$$
$$\mu_j \leq \kappa_j, \quad j = 1, \ldots, 39, \qquad (19d)$$
$$\mu_0^{(\ell)} = \rho_0^{(\ell)}, \quad \ell = 1, 2, 3, 4, \qquad (19e)$$

for $\epsilon = 10^{-2}$, and where $\tilde{\mu}_1$ and $\tilde{\mu}_2$ are given in Figure 2a; in particular, $\tilde{\mu}_2$ is a uniform distribution with the same total mass as the total distribution μ_j. Moreover, the species-dependent linear costs $\tilde{c}_\ell = c_{j,\ell}$, which we here take to be constant over time steps j, are given in Figure 2b. Finally, the capacity constraints κ_j, in (19d), are illustrated in Figure 2c. The multi-marginal optimal transport reformulation, which has a computational graph as illustrated in Figure 1a, is solved using Algorithm 1. The latter is adapted as in Remark 1 to handle both the costs on the total marginals in (19a) and the inequality constraints in (19d); details on the Fenchel duals of the functions involved are deferred to Appendix A. Results are shown in Figure 3, where the initial distributions $\rho_0^{(\ell)}$ for the different agents can be seen in the left-most column (showing time point $j = 0$). Note that the solution is relatively smooth, which is due to the smoothing effect from the noise term in the SDE (8), but with sharper characteristics around the edges of the spatially varying linear cost.

V. Conclusions and Future Directions

In this work, we present an efficient numerical algorithm for solving potential multi-species mean field games by utilizing the connection between potential mean field games and optimal transport. In particular, when reformulating the mean field game as an entropy-regularized multi-marginal optimal transport problem, the latter has a highly structured cost which can be utilized in order to develop an efficient numerical solution method. This is part of a larger framework of structured tensor optimization problems, which has applications in many different areas of control and estimation [22], [29], [30], [44]. In future work, we intend to relax the controllability assumption used here, and also relax the assumption that all species obey the same dynamics in order to allow for more heterogeneous sets of agents.

Appendix

A. Fenchel duals used in the numerical example

Let $x \in \mathbb{R}^N$, $A \subset \mathbb{R}^N$, and let $I_A(x)$ denote the indicator function on a set A, i.e., the function

$$I_A(x) := \begin{cases} 0, & \text{if } x \in A \\ \infty, & \text{else.} \end{cases}$$

Indicator functions can be used to impose constraints in minimization problems, since including $I_A(x)$ in the cost function is equivalent with imposing the constraint $x \in A$. Now, let $A = \{x \in \mathbb{R}^N \mid 0 \leq x \leq \hat{x}\}$ for some $\hat{x} \in \mathbb{R}_+^N$. The Fenchel dual of $g(x) = I_{\{0 \leq \cdot \leq \hat{x}\}}(x)$ is

$$g^*(y) = \sup_x \, \langle x, y \rangle - I_{\{0 \leq \cdot \leq \hat{x}\}}(x) = \langle \hat{x}, \max(y, 0) \rangle,$$

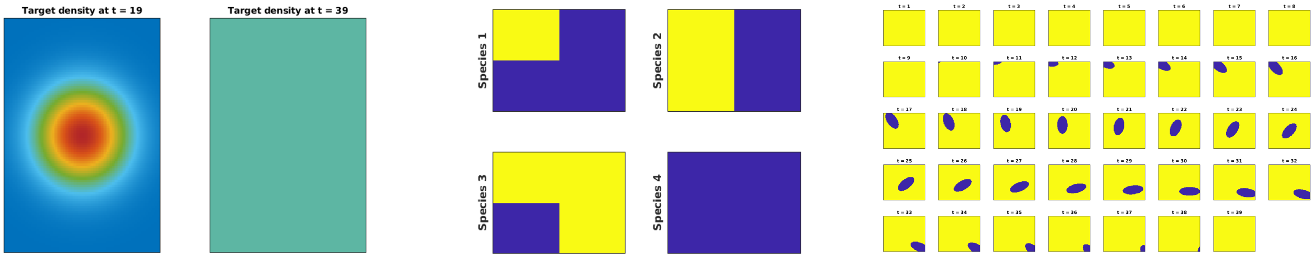

(a) Target densities at time points $j = 19$ and $j = 39$, for the total density.

(b) The linear cost $\tilde{c}_\ell$ for the different species; blue means cost 0, while yellow means a cost of $0.009 = 390\Delta x \Delta t$.

(c) The capacity constraints κ_j at the different time points; blue means zero (obstacle) while yellow means infinite capacity.

Fig. 2: Figures describing the setup in the numerical example in Section IV.

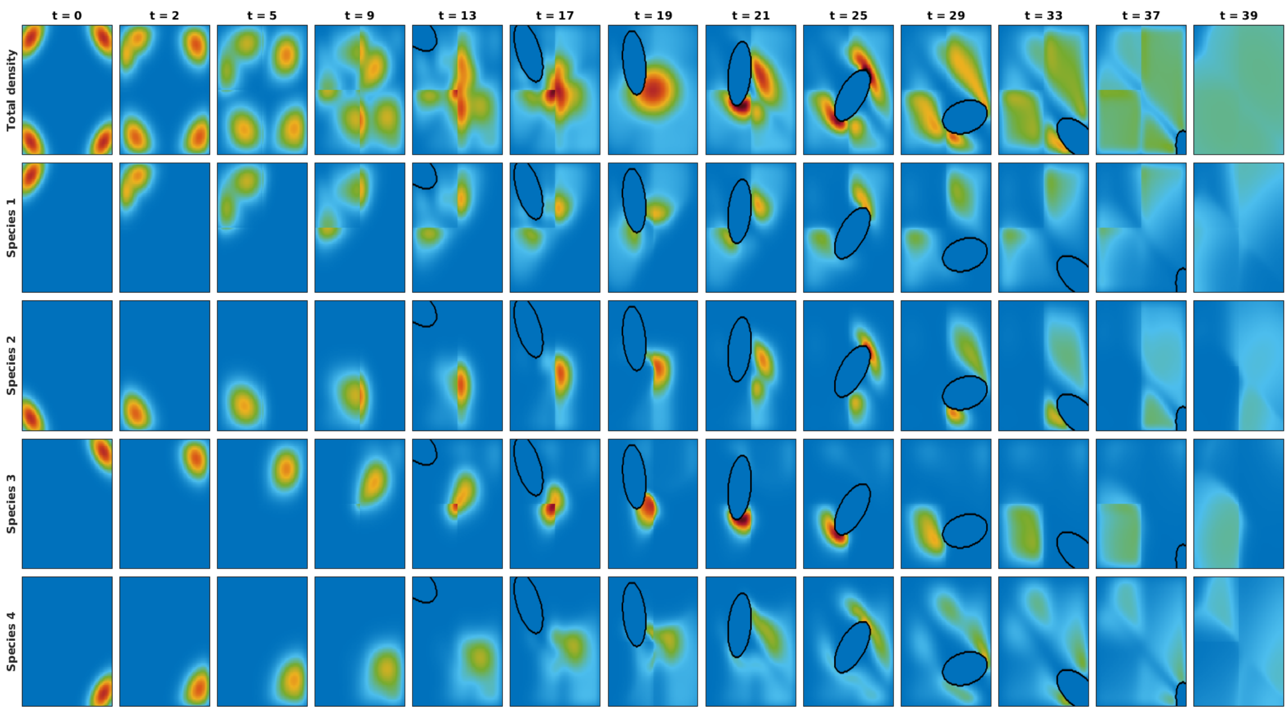

Fig. 3: Time evolution of total density and densities of the individual species, for the numerical example in Section IV.

with (sub)gradient given by

$$\nabla g^*(y) = \begin{cases} \hat{x}_i, & \text{if } y_i > 0 \\ 0, & \text{else.} \end{cases}$$

This means that the equations in (17) take the form

$$0 = -y \odot w + \nabla g^*(-\epsilon \log(y))$$

which has the solution $y = \max(w./\hat{x}, \mathbf{1})$, where the max is to be interpreted element-wise.

Next, let $x, z \in \mathbb{R}^N$, $\sigma \in \mathbb{R}_+$, and let $g(x) = \sigma\|x - z\|_2^2$. Then [3, Ex. 13.2.(i) and Prop. 13.22.(i)] gives that

$$g^*(y) = \frac{1}{4\sigma}\|y\|_2^2 + \langle z, y \rangle = \left\langle y, \frac{1}{4\sigma} y + z \right\rangle,$$

the gradient of which is given by

$$\nabla g^*(y) = \frac{1}{2\sigma} y + z.$$

The equations in (17) hence take the form

$$0 = -y \odot w - \frac{\epsilon}{2\sigma} \log(y) + z. \tag{20}$$

Such equations can be solved component-wise, by using that for scalars y, a, b, and c, we have that $ay + b\log(y) = c$ is equivalent with $\tilde{y} + \log(\frac{b}{a}\tilde{y}) - \log(\frac{b}{a}) = \frac{c}{b} - \log(\frac{b}{a})$, where $\tilde{y} = y\frac{a}{b}$. The latter leads to the equation $\tilde{y} + \log(\tilde{y}) = \frac{c}{b} - \log(\frac{b}{a})$ and therefore $y = \frac{b}{a}\,\omega(\frac{c}{b} - \log(\frac{b}{a}))$, where ω is the Wright omega function. The latter is defined as $\omega(x)$ being the solution to $y + \log(y) = x$, and is closely related to the Lambert W function, see, e.g., [18] and [17], respectively. In particular, the solution to (20) is therefore given by

$$y = \left(\frac{\epsilon}{2\sigma}\mathbf{1}./w\right) \odot \omega\left(\frac{2\sigma}{\epsilon} z - \log\left(\frac{\epsilon}{2\sigma}\mathbf{1}./w\right)\right).$$

References

[1] Y. Achdou, M. Bardi, and M. Cirant. Mean field games models of segregation. *Mathematical Models and Methods in Applied Sciences*, 27(01):75–113, 2017.

[2] J.M. Altschuler and E. Boix-Adsera. Polynomial-time algorithms for multimarginal optimal transport problems with structure. *arXiv preprint arXiv:2008.03006*, 2020.

[3] H.H. Bauschke and P.L. Combettes. *Convex analysis and monotone operator theory in Hilbert spaces*. Springer, Cham, 2nd edition, 2017.

[4] J.-D. Benamou and Y. Brenier. A computational fluid mechanics solution to the Monge-Kantorovich mass transfer problem. *Numerische Mathematik*, 84(3):375–393, 2000.

[5] J.-D. Benamou, G. Carlier, M. Cuturi, L. Nenna, and G. Peyré. Iterative Bregman projections for regularized transportation problems. *SIAM Journal on Scientific Computing*, 37(2):A1111–A1138, 2015.

[6] J.-D. Benamou, G. Carlier, S. Di Marino, and L. Nenna. An entropy minimization approach to second-order variational mean-field games. *Mathematical Models and Methods in Applied Sciences*, 29(08):1553–1583, 2019.

[7] A. Bensoussan, J. Frehse, and P. Yam. *Mean field games and mean field type control theory*. Springer, New York, NY, 2013.

[8] A. Bensoussan, T. Huang, and M. Laurière. Mean field control and mean field game models with several populations. *Minimax Theory and its Applications*, 3(2):173–209, 2018.

[9] P.E. Caines, M. Huang, and R.P. Malhamé. Mean field games. In T. Başar and G. Zaccour, editors, *Handbook of Dynamic Game Theory*, pages 345–372. Springer, Cham, 2018.

[10] P. Cardaliaguet, P.J. Graber, A. Porretta, and D. Tonon. Second order mean field games with degenerate diffusion and local coupling. *Nonlinear Differential Equations and Applications NoDEA*, 22(5):1287–1317, 2015.

[11] Y. Chen, T.T. Georgiou, and M. Pavon. On the relation between optimal transport and Schrödinger bridges: A stochastic control viewpoint. *Journal of Optimization Theory and Applications*, 169(2):671–691, 2016.

[12] Y. Chen, T.T. Georgiou, and M. Pavon. Optimal steering of a linear stochastic system to a final probability distribution, part I. *IEEE Transactions on Automatic Control*, 61(5):1158–1169, 2016.

[13] Y. Chen, T.T. Georgiou, and M. Pavon. Optimal transport over a linear dynamical system. *IEEE Transactions on Automatic Control*, 62(5):2137–2152, 2017.

[14] Y. Chen, T.T. Georgiou, and M. Pavon. Steering the distribution of agents in mean-field games system. *Journal of Optimization Theory and Applications*, 179(1):332–357, 2018.

[15] Y. Chen, T.T. Georgiou, and M. Pavon. Stochastic control liaisons: Richard Sinkhorn meets Gaspard Monge on a Schrödinger bridge. *SIAM Review*, 63(2):249–313, 2021.

[16] M. Cirant. Multi-population mean field games systems with Neumann boundary conditions. *Journal de Mathématiques Pures et Appliquées*, 103(5):1294–1315, 2015.

[17] R.M. Corless, G.H. Gonnet, D.E.G Hare, D.J. Jeffrey, and D.E. Knuth. On the Lambert W function. *Advances in Computational mathematics*, 5(1):329–359, 1996.

[18] R.M. Corless and D.J. Jeffrey. The Wright ω function. In *Artificial intelligence, automated reasoning, and symbolic computation*, pages 76–89. Springer, 2002.

[19] M. Cuturi. Sinkhorn distances: Lightspeed computation of optimal transport. In *Advances in Neural Information Processing Systems (NIPS)*, pages 2292–2300, 2013.

[20] P. Dai Pra. A stochastic control approach to reciprocal diffusion processes. *Applied mathematics and Optimization*, 23(1):313–329, 1991.

[21] B. Djehiche, A. Tcheukam, and H. Tembine. Mean-field-type games in engineering. *AIMS Electronics and Electrical Engineering*, 1(1):18–73, 2017.

[22] F. Elvander, I. Haasler, A. Jakobsson, and J. Karlsson. Multi-marginal optimal transport using partial information with applications in robust localization and sensor fusion. *Signal Processing*, 171:107474, 2020.

[23] W.H. Fleming and R.W. Rishel. *Deterministic and stochastic optimal control*. Springer-Verlag, New York, N.Y., 1975.

[24] H. Föllmer. Random fields and diffusion processes. In P.-L. Hennequin, editor, *École d'Été de Probabilités de Saint-Flour XV–XVII, 1985–87*, volume 1362 of *Lecture Notes in Mathematics*, pages 101–203. Springer, Berlin, Heidelberg, 1988.

[25] W. Gangbo and A. Świech. Optimal maps for the multidimensional Monge-Kantorovich problem. *Communications on Pure and Applied Mathematics: A Journal Issued by the Courant Institute of Mathematical Sciences*, 51(1):23–45, 1998.

[26] I. Gentil, C. Léonard, and L. Ripani. About the analogy between optimal transport and minimal entropy. *Annales de la Faculté des sciences de Toulouse: Mathématiques*, 26(3):569–600, 2017.

[27] I. Haasler, Y. Chen, and J. Karlsson. Optimal steering of ensembles with origin-destination constraints. *IEEE Control Systems Letters*, 5(3):881–886, 2020.

[28] I. Haasler, A. Ringh, Y. Chen, and J. Karlsson. Estimating ensemble flows on a hidden Markov chain. In *2019 IEEE 58th Conference on Decision and Control (CDC)*, pages 1331–1338. IEEE, 2019.

[29] I. Haasler, A. Ringh, Y. Chen, and J. Karlsson. Multimarginal optimal transport with a tree-structured cost and the Schrödinger bridge problem. *SIAM Journal on Control and Optimization*, 59(4):2428–2453, 2021.

[30] I. Haasler, A. Ringh, Y. Chen, and J. Karlsson. Scalable computation of dynamic flow problems via multi-marginal graph-structured optimal transport. *arXiv preprint arXiv:2106.14485v1*, 2021.

[31] I. Haasler, R. Singh, Q. Zhang, J. Karlsson, and Y. Chen. Multi-marginal optimal transport and probabilistic graphical models. *IEEE Transactions on Information Theory*, 67(7):4647–4668, 2021.

[32] A. Hindawi, J.-B. Pomet, and L. Rifford. Mass transportation with LQ cost functions. *Acta applicandae mathematicae*, 113(2):215–229, 2011.

[33] M. Huang, P.E. Caines, and R.P. Malhamé. Social optima in mean field LQG control: centralized and decentralized strategies. *IEEE Transactions on Automatic Control*, 57(7):1736–1751, 2012.

[34] M. Huang, R.P. Malhamé, and P.E. Caines. Large population stochastic dynamic games: closed-loop McKean-Vlasov systems and the Nash certainty equivalence principle. *Communications in Information & Systems*, 6(3):221–252, 2006.

[35] B. Jovanovic and R.W. Rosenthal. Anonymous sequential games. *Journal of Mathematical Economics*, 17(1):77–87, 1988.

[36] J. Karlsson and A. Ringh. Generalized Sinkhorn iterations for regularizing inverse problems using optimal mass transport. *SIAM Journal on Imaging Sciences*, 10(4):1935–1962, 2017.

[37] A. Lachapelle and M.-T. Wolfram. On a mean field game approach modeling congestion and aversion in pedestrian crowds. *Transportation research part B: methodological*, 45(10):1572–1589, 2011.

[38] B. Lamond and N.F. Stewart. Bregman's balancing method. *Transportation Research Part B: Methodological*, 15(4):239–248, 1981.

[39] J.-M. Lasry and P.-L. Lions. Mean field games. *Japanese journal of mathematics*, 2(1):229–260, 2007.

[40] Z.-Q. Luo and P. Tseng. On the convergence of the coordinate descent method for convex differentiable minimization. *Journal of Optimization Theory and Applications*, 72(1):7–35, 1992.

[41] L. Nenna. *Numerical methods for multi-marginal optimal transportation*. PhD thesis, PSL Research University, 2016.

[42] B. Pass. Multi-marginal optimal transport: theory and applications. *ESAIM: Mathematical Modelling and Numerical Analysis*, 49(6):1771–1790, 2015.

[43] G. Peyré and M. Cuturi. Computational optimal transport: With applications to data science. *Foundations and Trends® in Machine Learning*, 11(5-6):355–607, 2019.

[44] A. Ringh, I. Haasler, Y. Chen, and J. Karlsson. Graph-structured tensor optimization for nonlinear density control and mean field games. *In preparation*, 2021.

[45] L. Rüschendorf. Optimal solutions of multivariate coupling problems. *Applicationes Mathematicae*, 23(3):325–338, 1995.

[46] L. Rüschendorf and L. Uckelmann. On the n-coupling problem. *Journal of multivariate analysis*, 81(2):242–258, 2002.

[47] R. Singh, I. Haasler, Q. Zhang, J. Karlsson, and Y. Chen. Inference with aggregate data: An optimal transport approach. *arXiv preprint arXiv:2003.13933*, 2020.

[48] P. Tseng. Dual ascent methods for problems with strictly convex costs and linear constraints: A unified approach. *SIAM Journal on Control and Optimization*, 28(1):214–242, 1990.

[49] C. Villani. *Topics in optimal transportation*. American Mathematical Society, Providence, RI, 2003.